# Imidazolium-Based Ionic Liquids Affect Morphology and Rigidity of Living Cells: an Atomic Force Microscopy Study

Massimiliano Galluzzi[1,2], Carsten Schulte[2], Paolo Milani[2], Alessandro Podestà[2]*

[1] Shenzhen Key Laboratory of Nanobiomechanics, Shenzhen Institutes of Advanced Technology, Chinese Academy of Sciences, Shenzhen 518055, Guangdong, China.

[2] C.I.Ma.I.Na and Dipartimento di Fisica "Aldo Pontremoli", Università degli Studi di Milano, via Celoria 16, 20133 - Milano, Italy.

* Corresponding author: Prof. Alessandro Podestà, e-mail: alessandro.podesta@mi.infn.it

## SUPPORTING INFORMATION

## Table of Contents

## Details of the analysis of force curves

**Finite thickness correction.** A requisite for the validity of the Hertz model is that the indentation is small compared to the thickness of the sample. When this condition is not satisfied, and the probe is indenting an elastic thin film supported by a hard surface, the material appears stiffer, due to the spatial confinement of the strain and stress fields. A safe condition is that the thickness should exceed by a factor of more than ten the indentation (for examples, see the difference in the F vs. indentation curves in Figure S1e). Dimitriadis et al.[1] proposed a correction for the finite thickness effect that can be applied to force-indentation curves acquired using spherical tips. This correction is working with two different boundary conditions: bound cells (i.e. well adherent), and not bound cells. Since cells spread and adhere on substrate through highly dynamic focal adhesions points, a reasonable boundary condition for cells is in between the bound and not bound limiting conditions. If one uses the arithmetical mean of the coefficients for bound and not bound states, the following equation for the Hertz equation is obtained:[2]

$$F = \frac{4}{3}\frac{E\sqrt{R}}{(1-\nu^2)}\delta^{3/2}[1 + 1.009\chi_S + 1.032{\chi_S}^2 + 0.578{\chi_S}^3 + 0.0048{\chi_S}^4] \qquad \text{(S1)}$$

where the correction factor does depend on indentation, through the adimensional parameter $\chi_S = \sqrt{R\delta}/h$ (for spherical probes). h is the local sample thickness at zero force, i.e. the real thickness, from the uncompressed topographic map. Remarkably, the numerator in $\chi_s$ represents the radius of the contact area, which is larger for colloidal probes than for standard sharp AFM tips.

The above model assumes that the sample surface is flat on a scale significantly larger than that of the indenter. The local inclination across the cell is almost everywhere rather mild on the scale of the colloidal probe, with the exception of the extreme peripheral regions. To minimize artifacts, we typically applied a mask based on topography to filter off the extreme cell-substrate boundary region, where obvious artifacts are present. Therefore, the impact of local inclination on the accuracy of finite thickness correction is likely irrelevant, compared to the other sources of error, in particular when considering shallow indentations.

**Stability of the cell sample over time.** Only minor modifications in morphological and mechanical properties of cells are evidenced in Figure S1. Living cells (especially the MDA-MB-231 cell line derived from metastatic cancerous tissues) move, spread and reorganize their cytoskeletal structure during the measurements (20 min for a single FV; total time for the data presented in Figure S1 was 2 h).

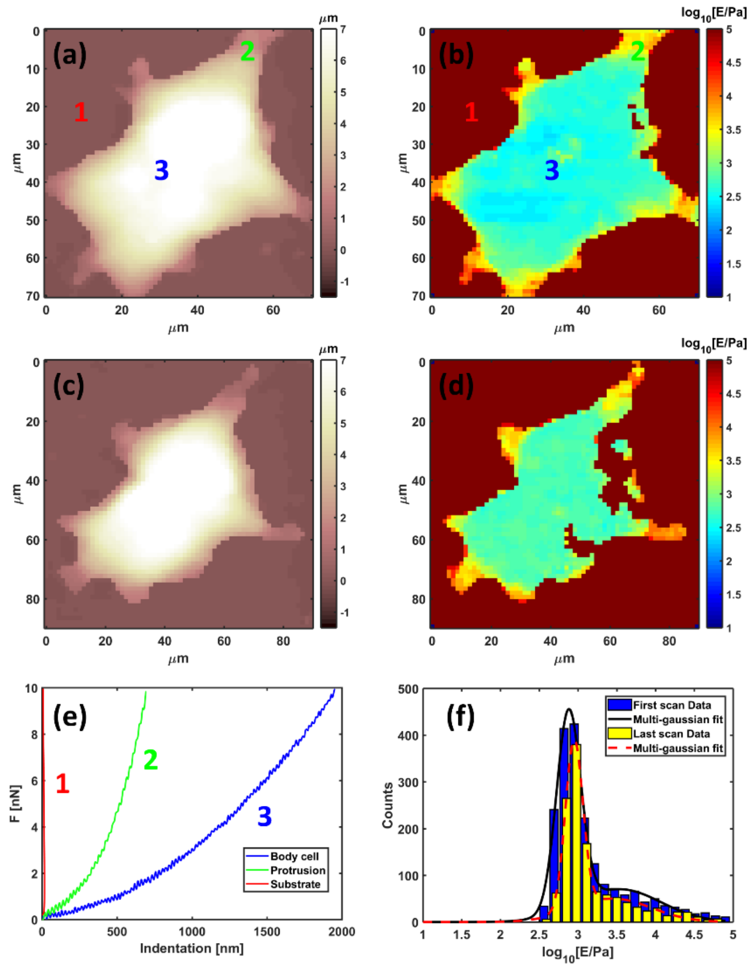


**Figure S1. Evolution of morphology and Young's modulus (with finite thickness correction) for a selected MDA-MB-231 cells. Images (a) and (b) represent the initial morphology and Young's modulus map, while images (c) and (d) represent final morphology and Young's modulus map after six consecutive FV analysis (20 min each). Graph (e) shows uncorrected representative Force vs. Indentation curves on substrate (1), protrusion (2) and cell body (3), also highlighted in (a) and (b). Finally, (f) represents the quantitative analysis through histograms and multi-Gaussian fit of Young's modulus values from maps (b) and (d).**

## Adhesion force on cells is negligible.

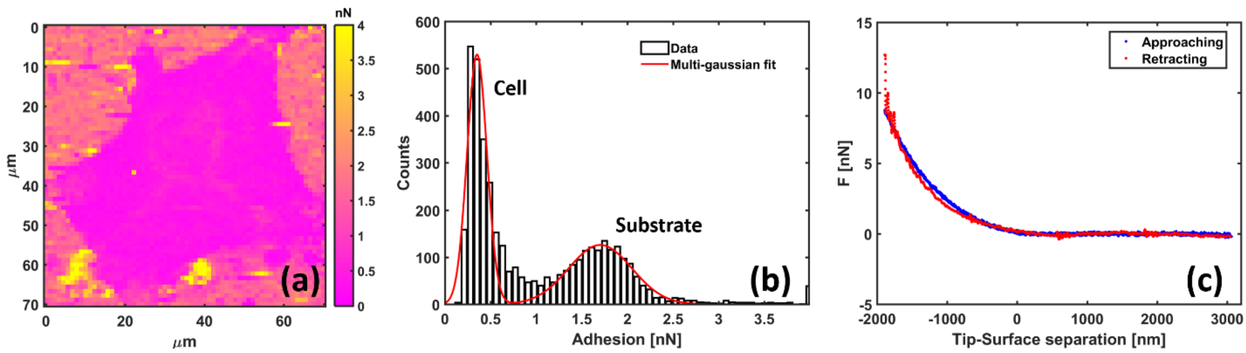


**Figure S2. Representative adhesion analysis for a selected MDA-MB-231 cell (from Figure S1). (a) Adhesion map obtained evaluating the adhesion well for each retracting curves. (b) Histograms and multi-Gaussian fit of the adhesion force values. (c) A representative force curve (approaching + retracting) showing the absence of the adhesion well (and also very minor hysteresis between approaching and retracting curves, usually related to viscoelastic effects).**

## $EC_{50}$ values of the selected ILs

| $EC_{50}$ (μM) | Phospho bact[3] | IPC-81[4] | A549[5] | HeLa[6] |
|---|---|---|---|---|
| **[$C_4$MIM][Cl]** | 2190 | 3550 | 11800 | 2300[a] |
| **[$C_4$MIM][$BF_4$]** | 1270 | 1320 | 73780 | 4500 |
| **[$C_8$MIM][Cl]** | 15 | 100 | 540 | 300[a] |

**Table S1. EC50 values (in μM units) for different cell lines and bacteria. ([a]) Data are presented using anion $[Br]^-$ in place of $[Cl]^-$.**

## Volume analysis of MDA-MB-231 cells

| Concentration | Single Cell Volume [$\mu m^3$] | | | Cell Volume Variation [%] | | |
|---|---|---|---|---|---|---|
| [mM][a], [μM][b] | **[$C_4$MIM][Cl][a]** | **[$C_4$MIM][$BF_4$] [a]** | **[$C_8$MIM][Cl] [b]** | **[$C_4$MIM][Cl] [a]** | **[$C_4$MIM][$BF_4$] [a]** | **[$C_8$MIM][Cl][b]** |
| none | 5910 | 8060 | 3610 | // | // | // |
| 1 | 6450 | 7710 | 3760 | +9 | -4 | +4 |
| 10 | 5540 | 7210 | 3750 | -6 | -10 | +4 |
| 100 | 3670 | 5080 | 3570 | -38 | -37 | -1 |

**Table S2. Cell volumes calculated from AFM morphologies of Figures 1-3 in the main text.**

# AFM data collection

**Data S1. MDA-MB-231 cells vs [$C_4$MIM][Cl]**

| IL conc. | Real Morphology | Mechanical map |
|---|---|---|
| None | 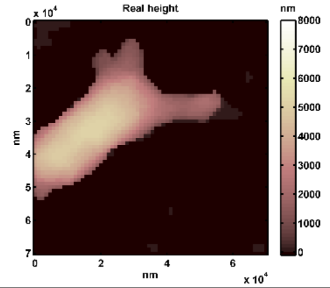 | 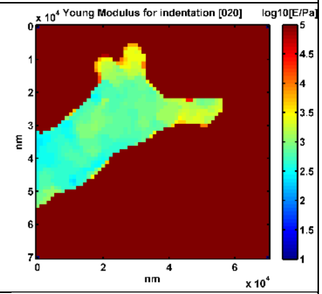 |
| none | 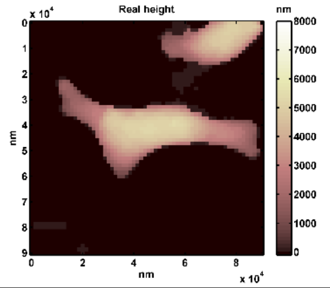 | 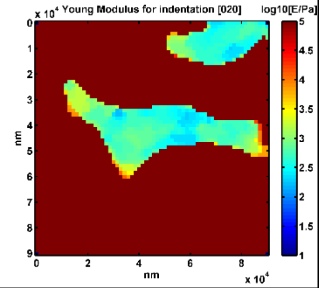 |
| none | 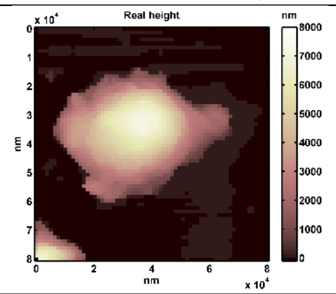 | 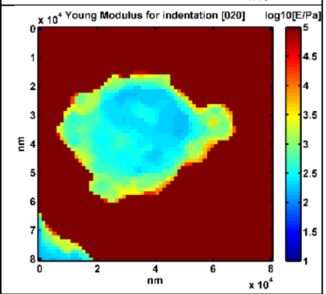 |
| none | 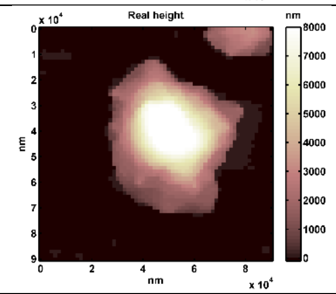 | 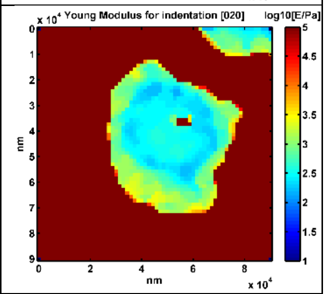 |
| none | 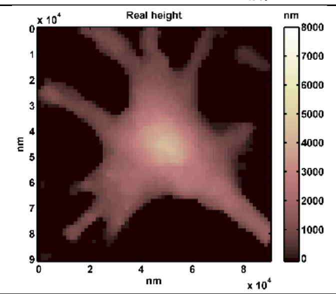 | 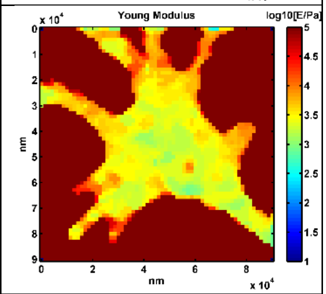 |

none

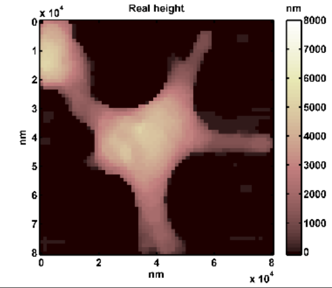


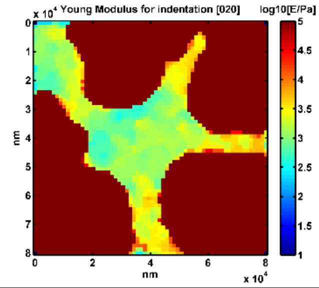


none

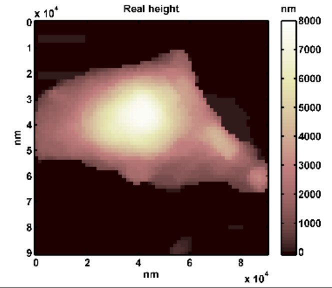


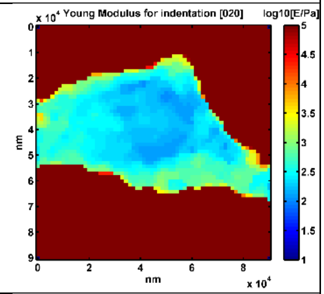


none

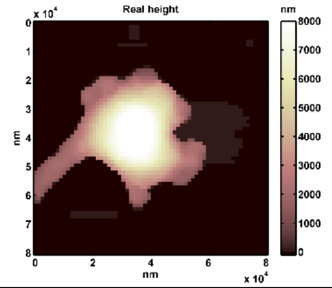


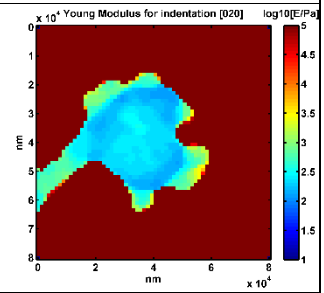


1 mM

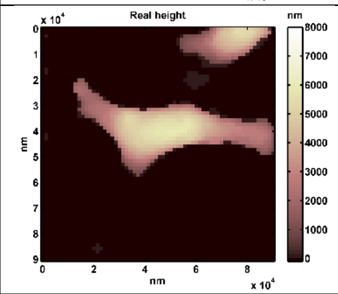


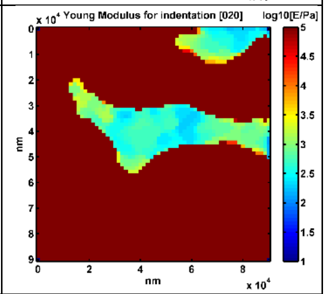


1 mM

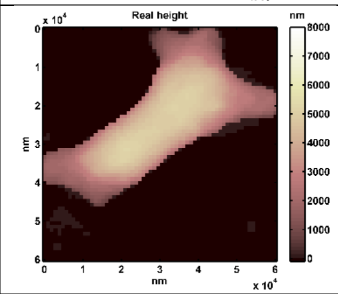


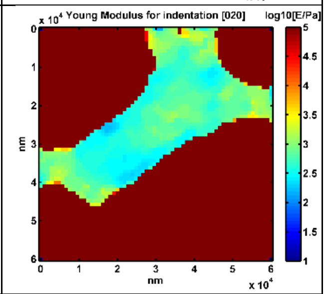


1 mM

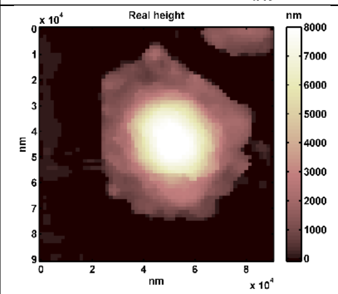


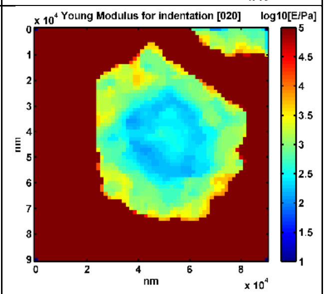

1 mM

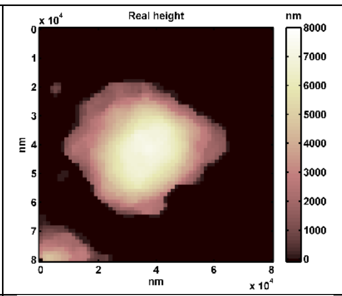


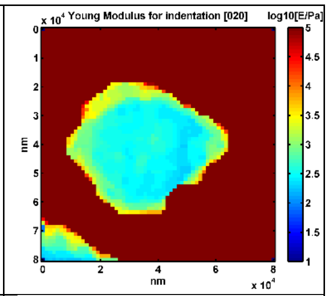


1 mM

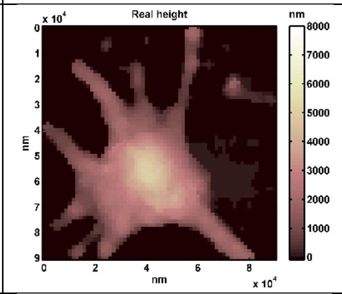


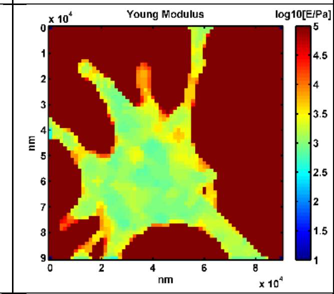


1 mM

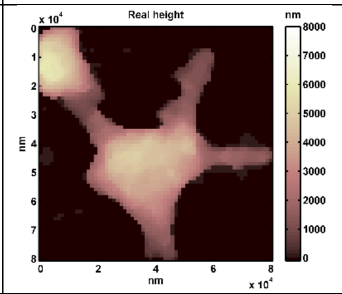


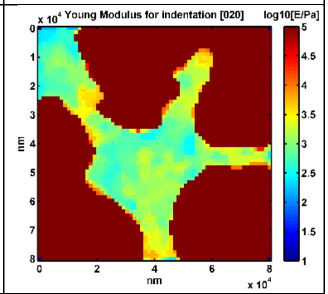


1 mM

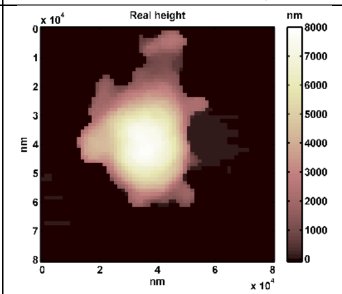


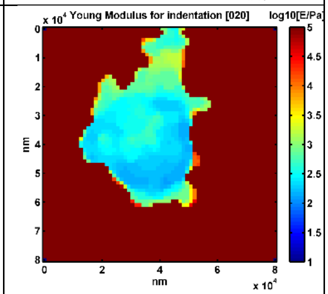


1 mM

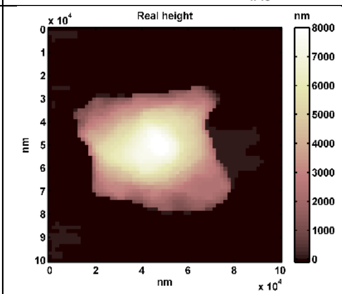


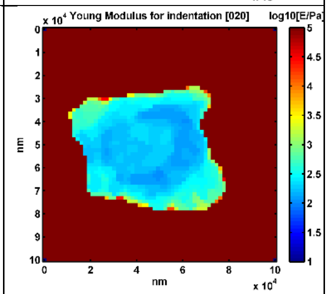


10 mM

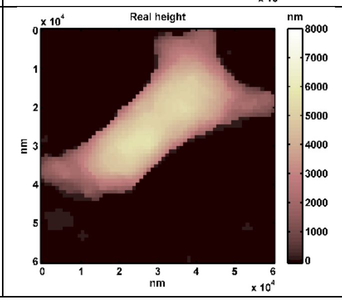


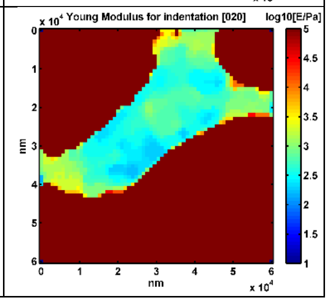

10 mM

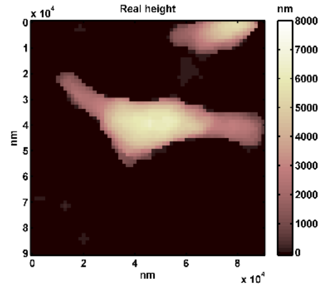


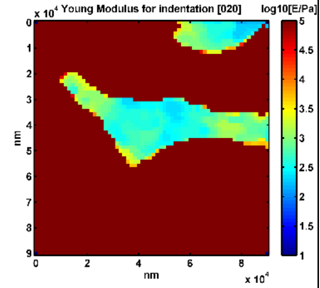


10 mM

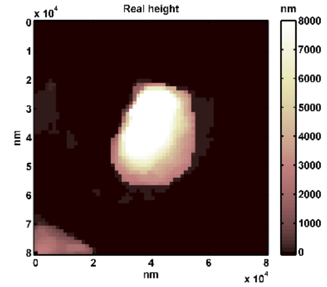


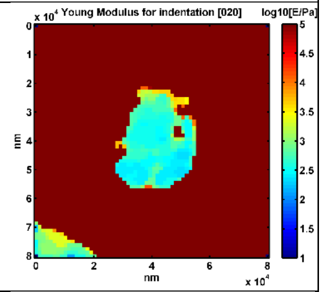


10 mM

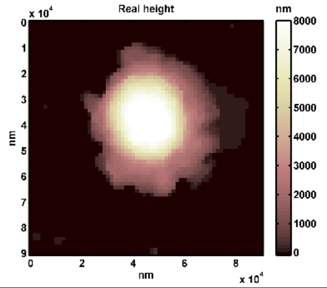


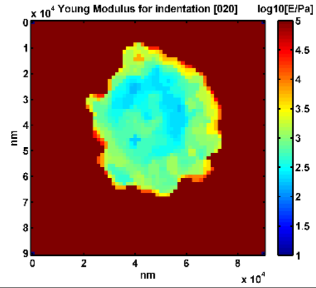


10 mM

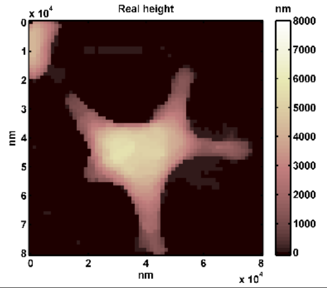


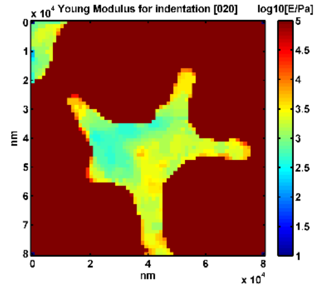


10 mM

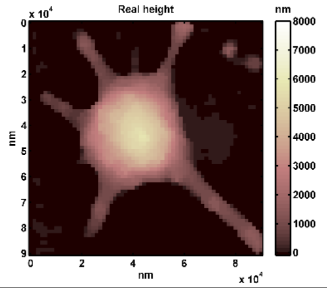


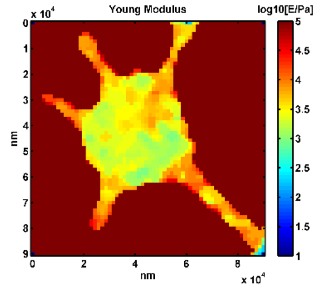


10 mM

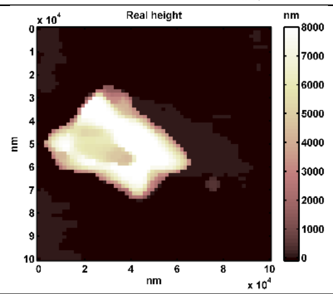


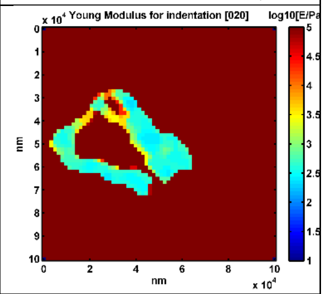

| | | |
|---|---|---|
| 10 mM | 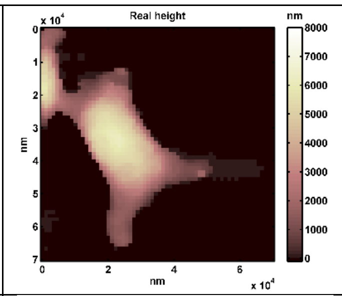 | 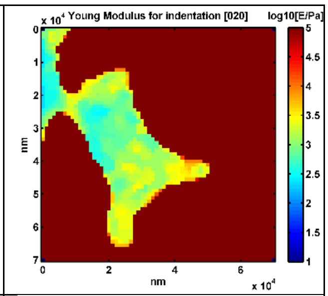 |
| 100 mM | 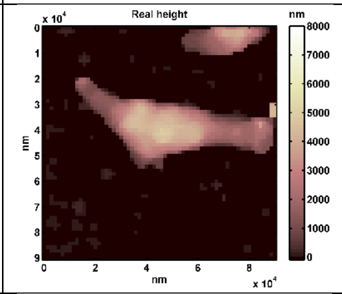 | 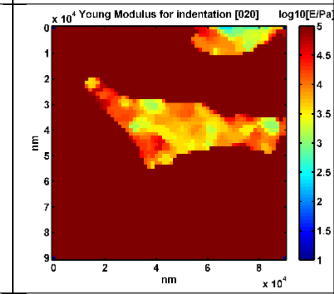 |
| 100 mM | 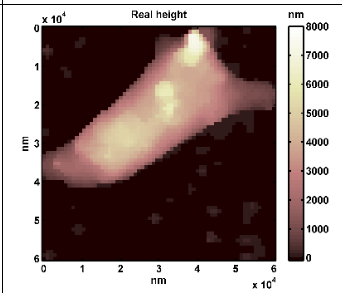 | 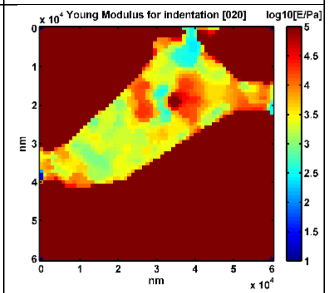 |
| 100 mM | 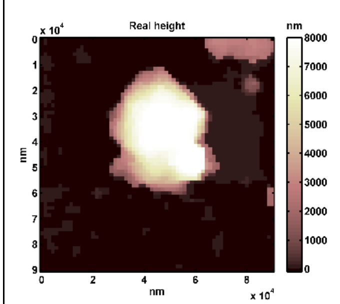 | 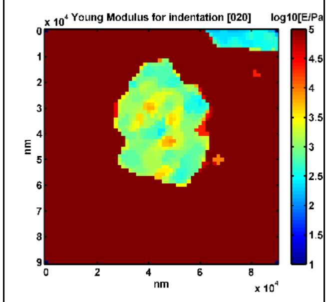 |
| 100 mM | 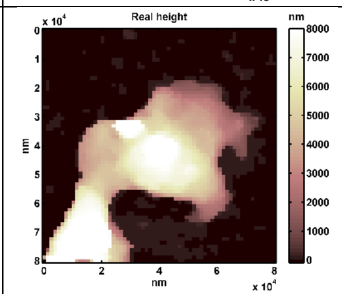 | 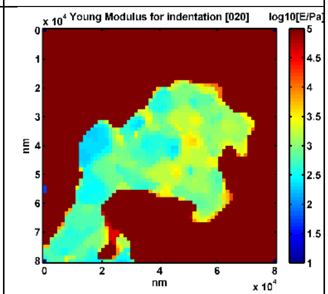 |
| 100 mM | 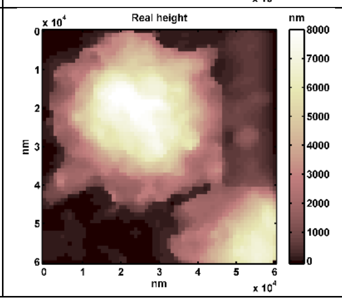 | 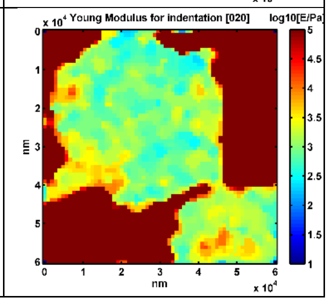 |

| | | |
|---|---|---|
| 100 mM | 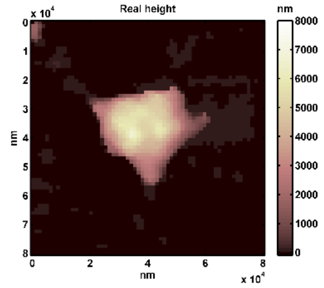 | 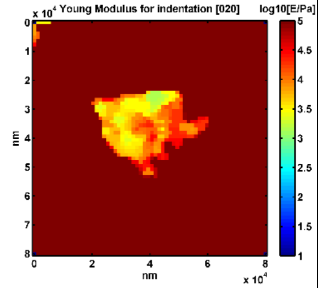 |
| 100 mM | 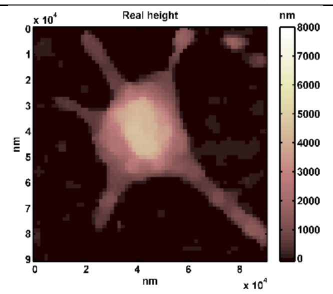 | 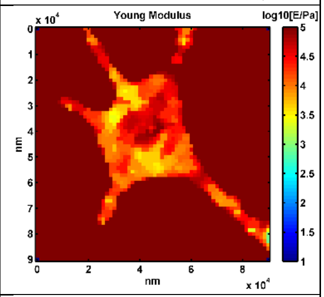 |
| 100 mM | 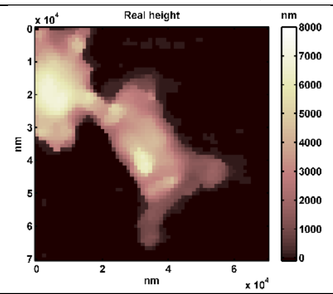 | 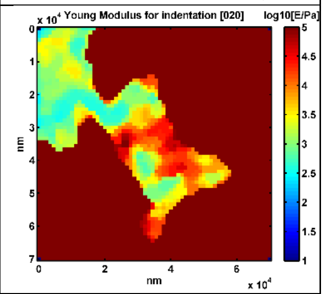 |

**Data S2. MDA-MB-231 cells vs [$C_4$MIM][$BF_4$]**

| **IL conc.** | **Real Morphology** | **Mechanical map** |
|---|---|---|
| None | 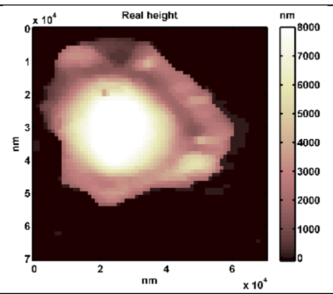 | 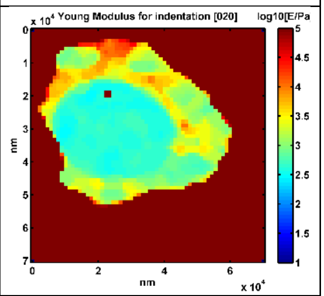 |
| none | 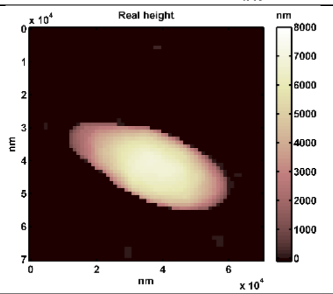 | 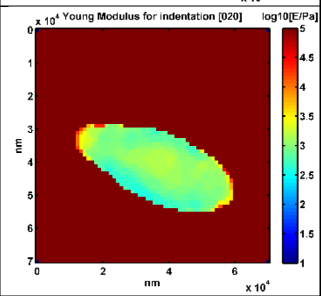 |

| | | |
|---|---|---|
| none | 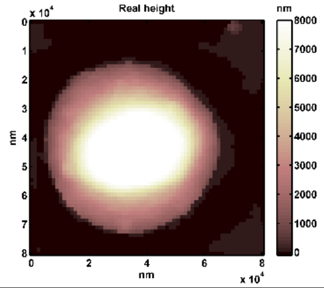  | 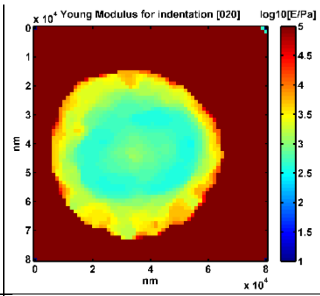  |
| none | 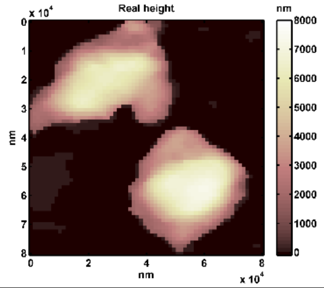  | 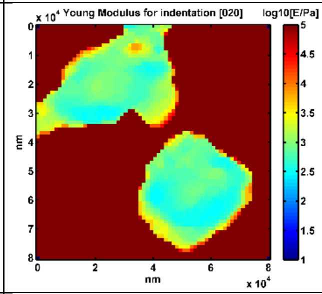  |
| none | 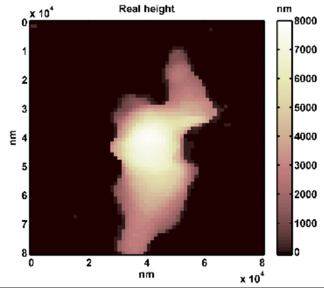  | 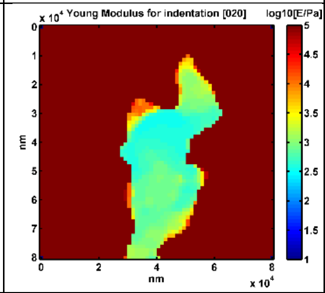  |
| none | 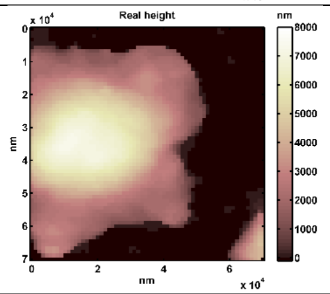  | 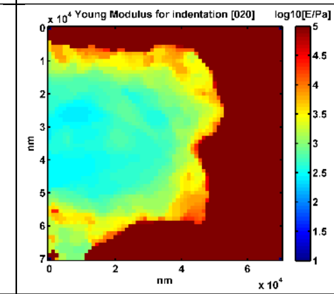  |
| none | 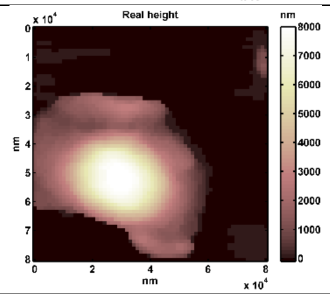  | 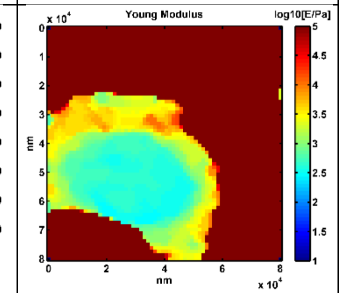  |
| none | 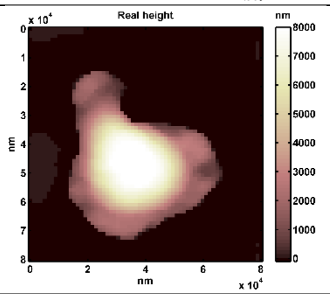  | 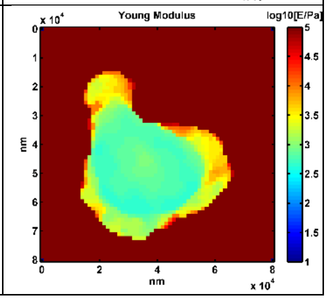  |

<table>
<tr><td>none</td><td>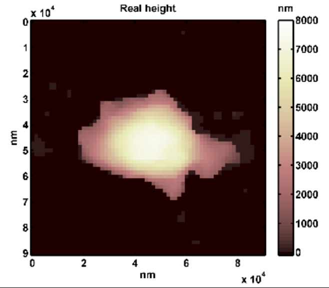
</td><td>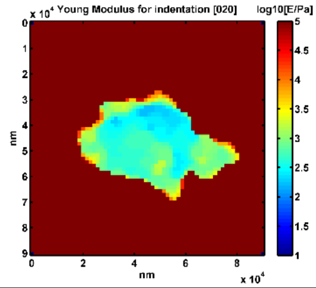
</td></tr>
<tr><td>none</td><td>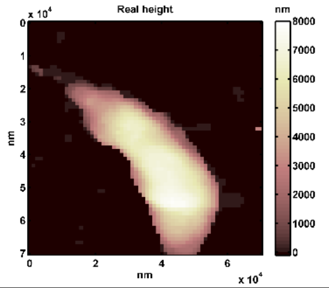
</td><td>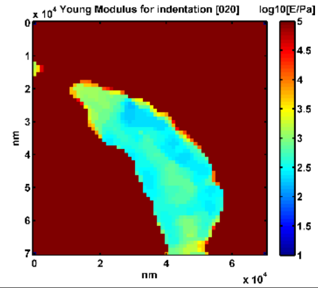
</td></tr>
<tr><td>none</td><td>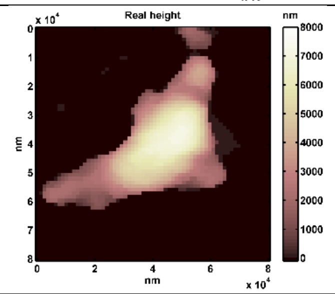
</td><td>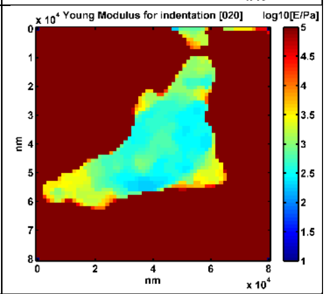
</td></tr>
<tr><td>none</td><td>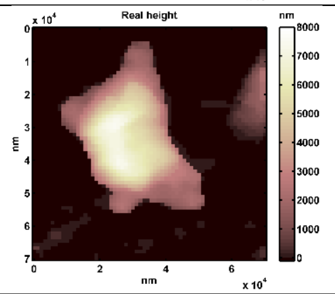
</td><td>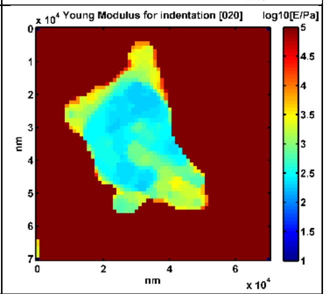
</td></tr>
<tr><td>none</td><td>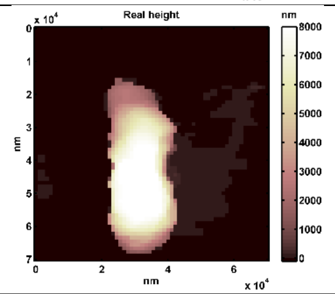
</td><td>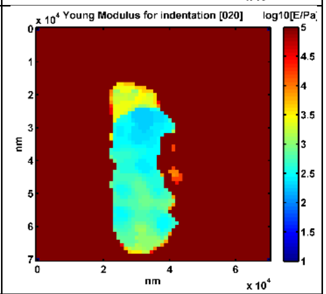
</td></tr>
<tr><td>1 mM</td><td>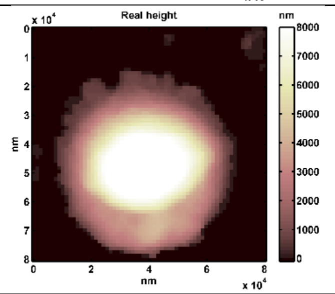
</td><td>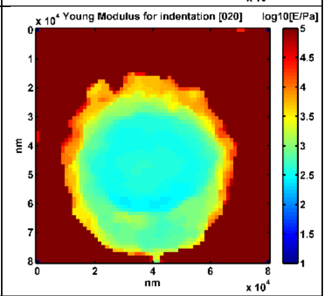
</td></tr>
</table>

| | | |
|---|---|---|
| 1 mM | 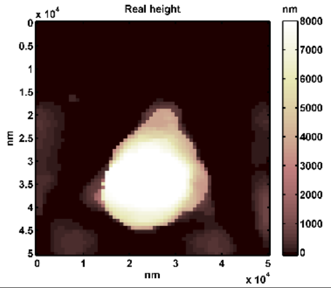 | 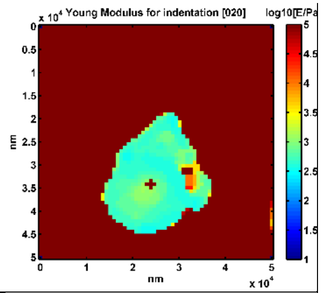 |
| 1 mM | 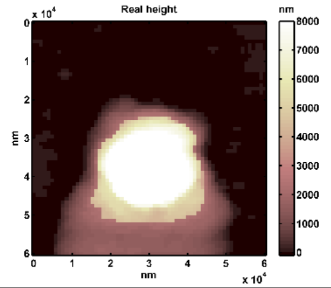 | 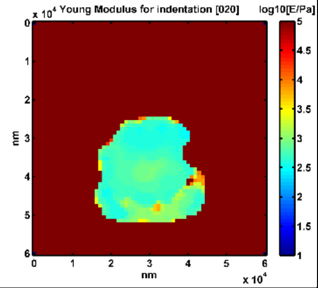 |
| 1 mM | 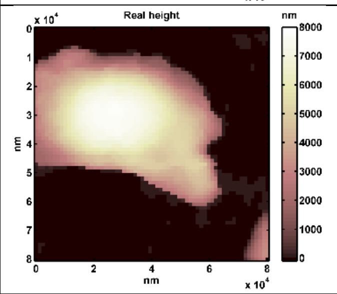 | 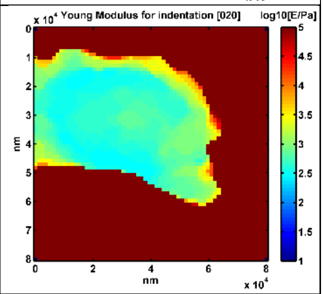 |
| 1 mM | 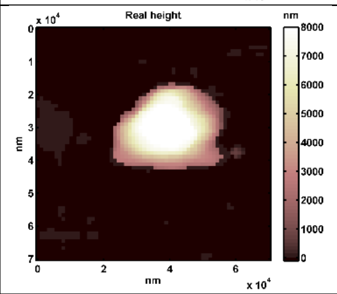 | 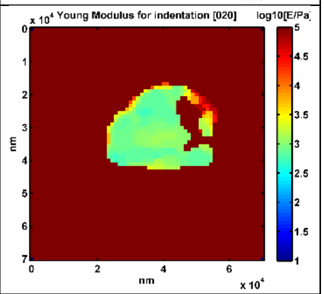 |
| 1 mM | 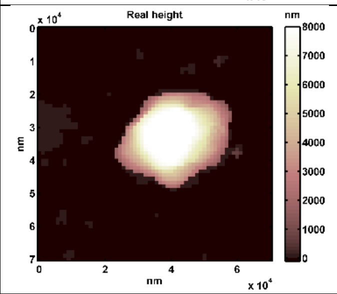 | 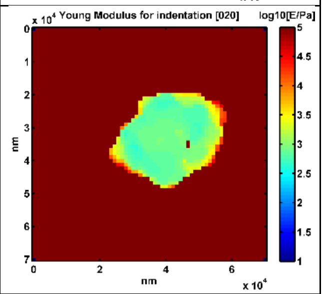 |
| 1 mM | 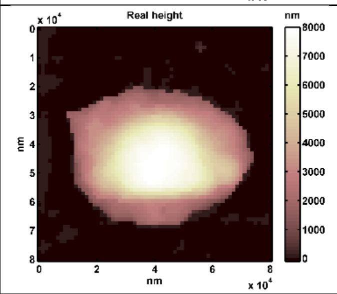 | 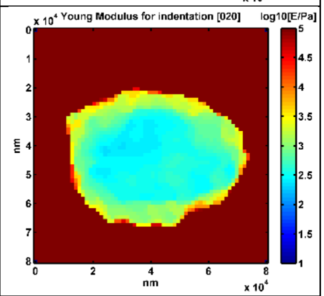 |

| | | |
|---|---|---|
| 1 mM | 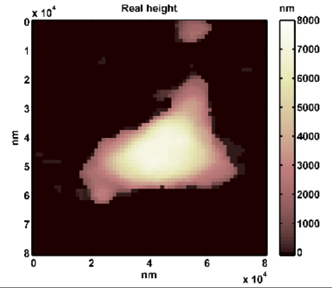 | 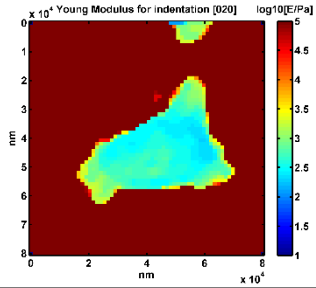 |
| 1 mM | 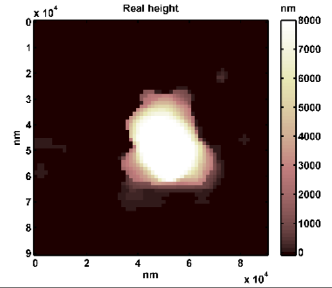 | 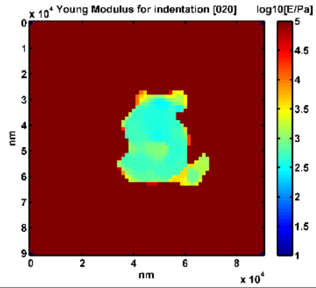 |
| 1 mM | 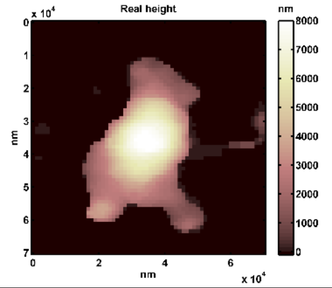 | 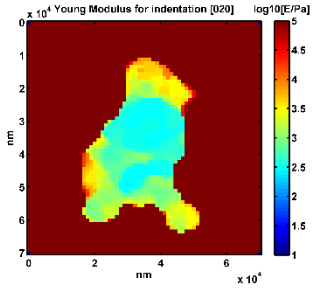 |
| 1 mM | 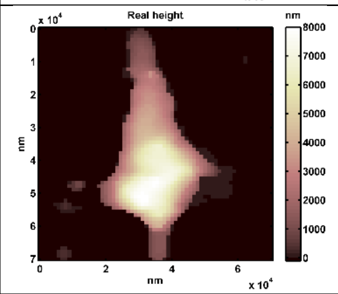 | 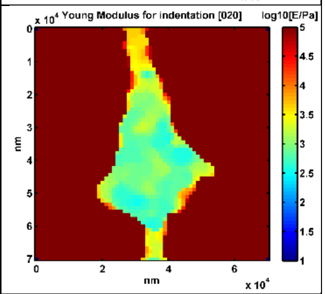 |
| 10 mM | 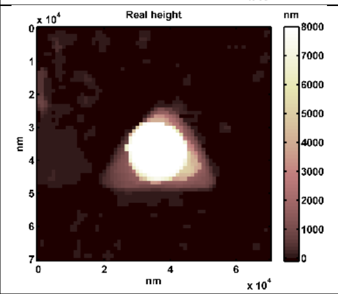 | 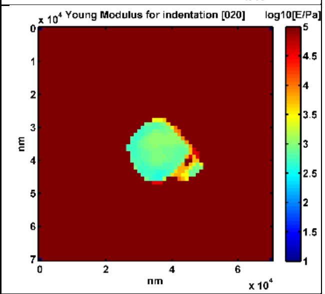 |
| 10 mM | 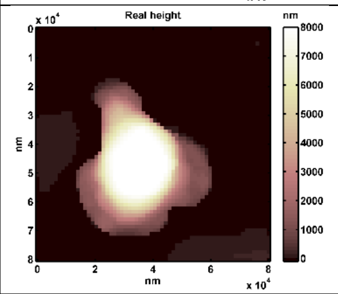 | 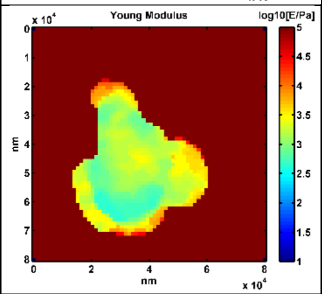 |

| | | |
|---|---|---|
| 10 mM | 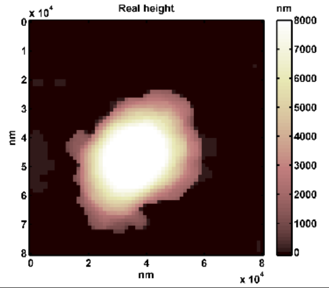  | 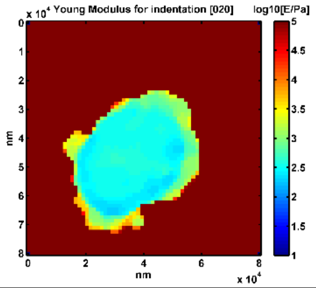  |
| 10 mM | 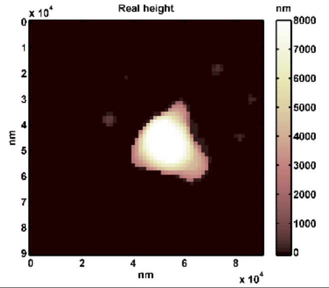  | 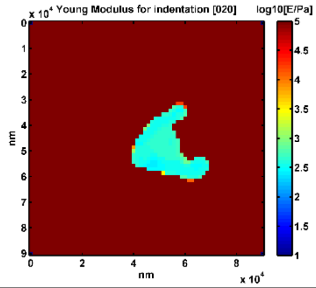  |
| 10 mM | 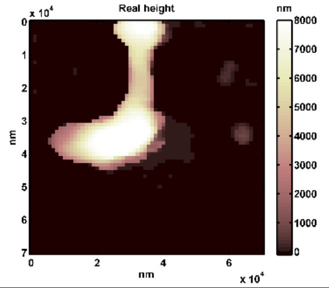  | 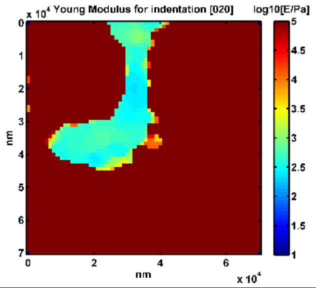  |
| 10 mM | 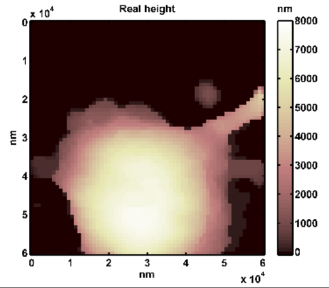  | 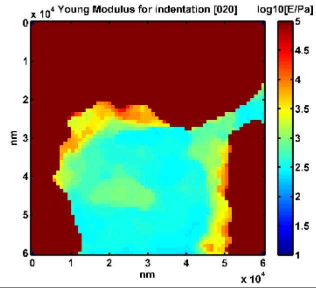  |
| 100 mM | 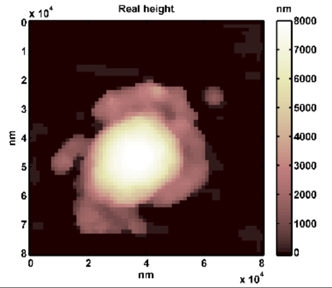  | 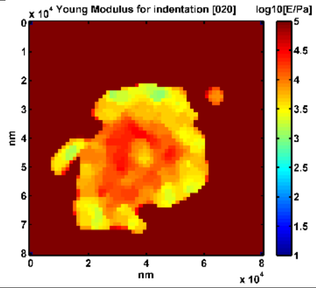  |
| 100 mM | 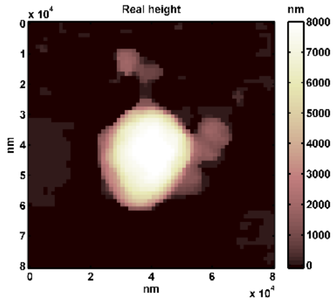  | 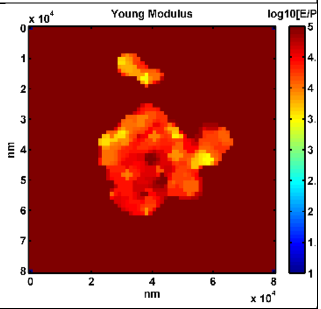  |

| | | |
|---|---|---|
| 100 mM | 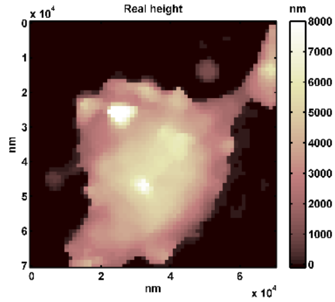  | 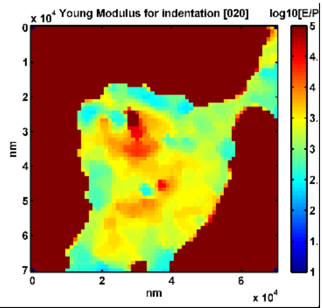  |
| 100 mM | 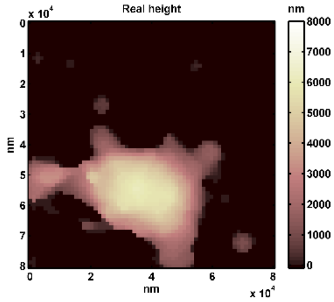  | 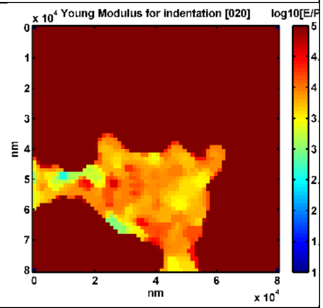  |

**Data S3. MDA-MB-231 cells vs [C$_8$MIM][Cl]**

| IL conc. | Real Morphology | Mechanical map |
|---|---|---|
| none | 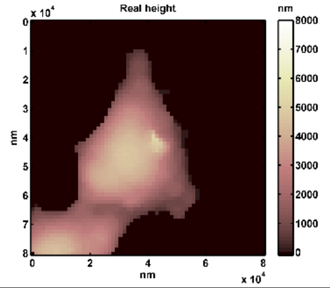  | 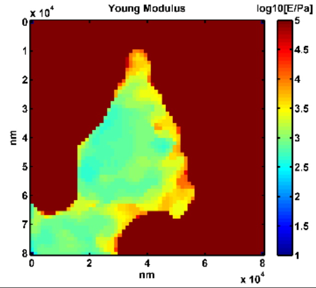  |
| none | 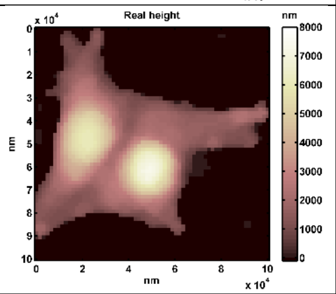  | 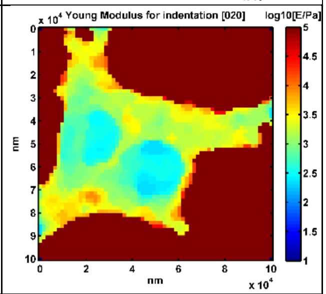  |
| none | 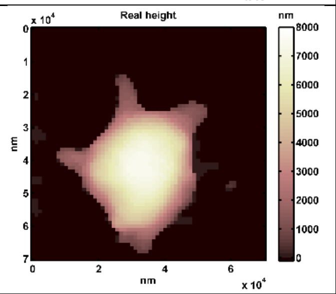  | 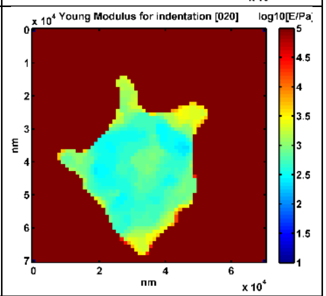  |

| | | |
|---|---|---|
| none | 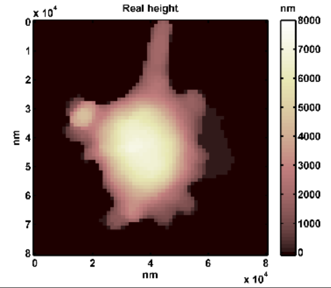 | 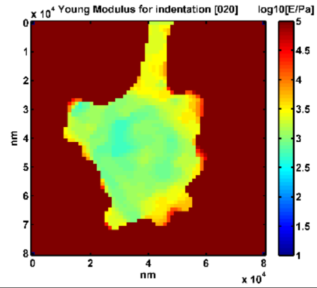 |
| +none | 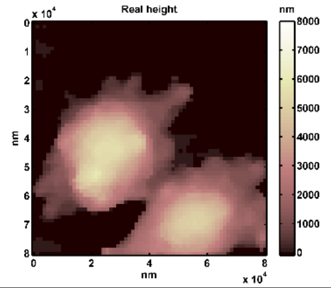 | 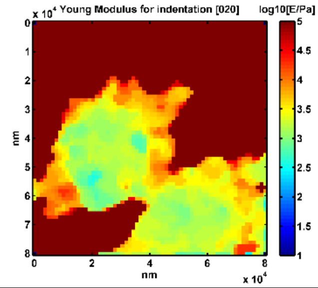 |
| none | 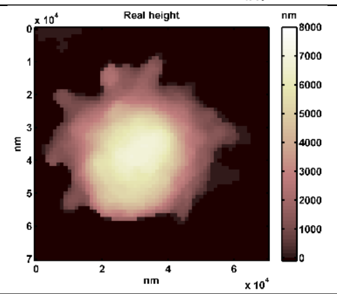 | 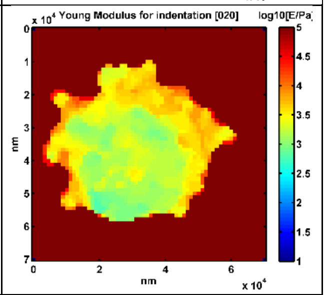 |
| none | 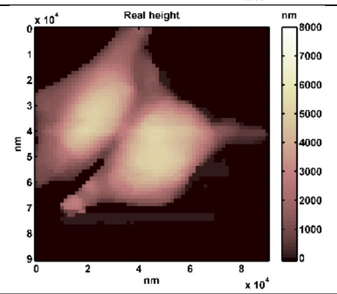 | 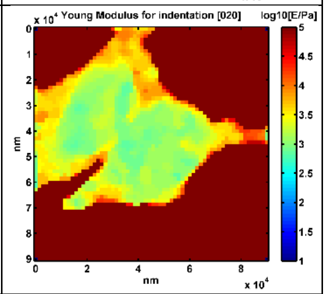 |
| none | 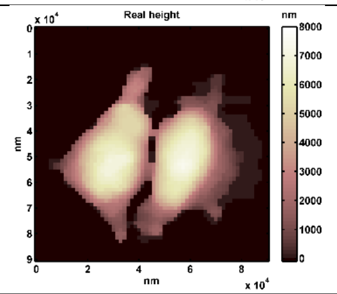 | 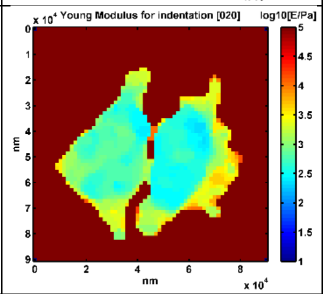 |
| 1 µM | 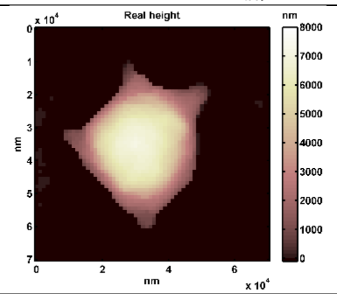 | 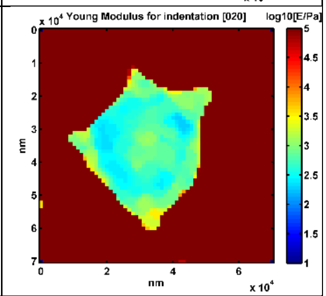 |

| | | |
|---|---|---|
| 1 µM | 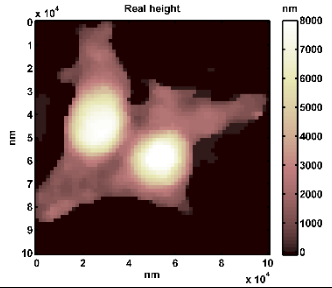  | 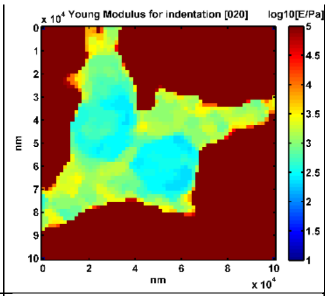  |
| 1 µM | 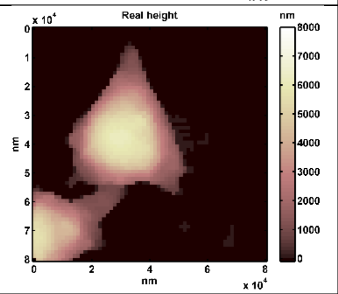  | 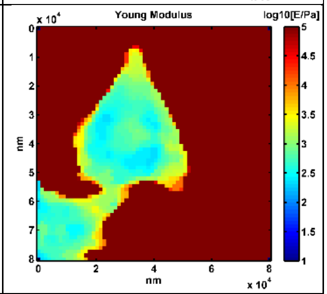  |
| 1 µM | 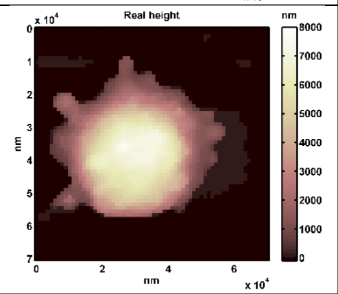  | 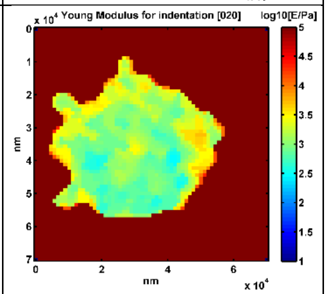  |
| 1 µM | 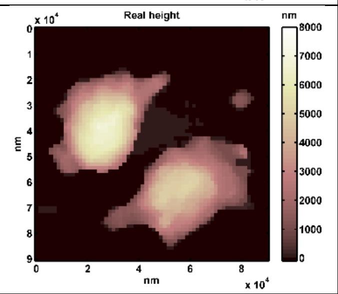  | 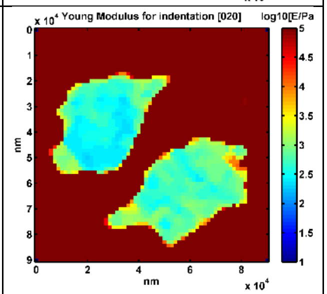  |
| 1 µM | 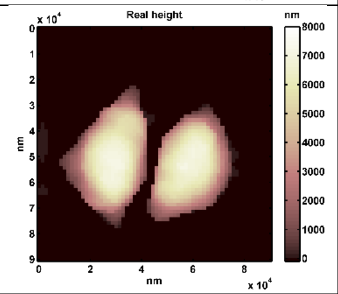  | 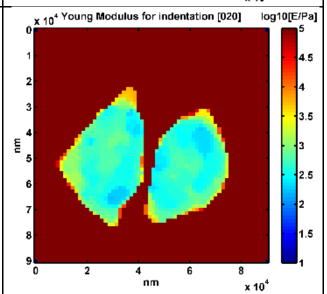  |
| 1 µM | 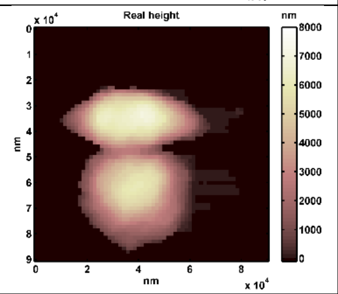  | 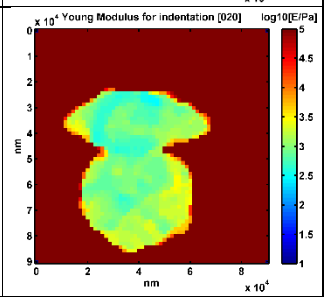  |

| | | |
|---|---|---|
| 10 μM | 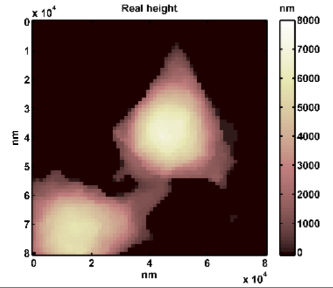  | 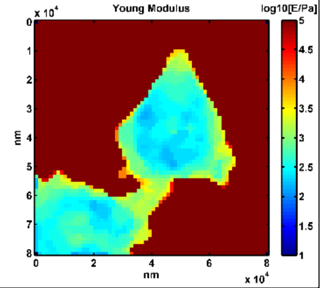  |
| 10 μM | 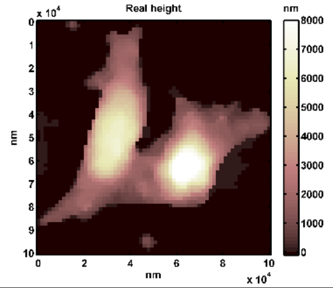  | 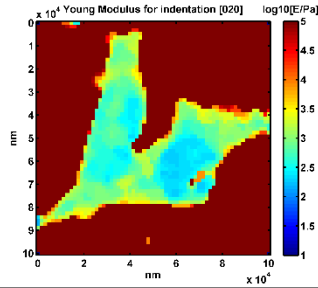  |
| 10 μM | 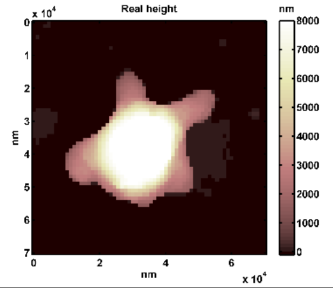  | 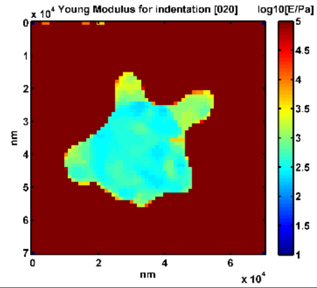  |
| 10 μM | 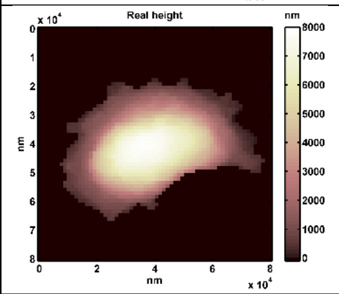  | 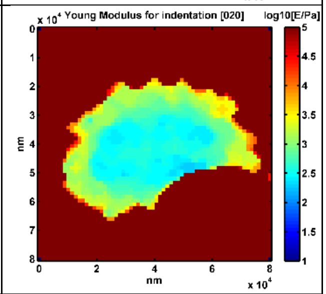  |
| 10 μM | 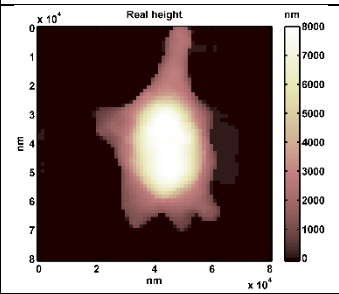  | 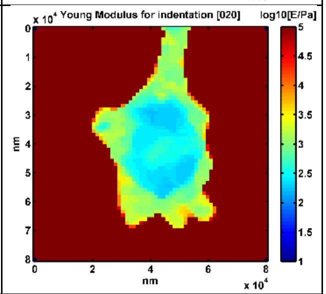  |
| 10 μM | 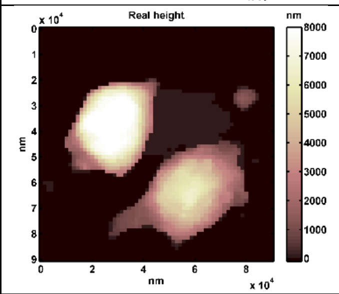  | 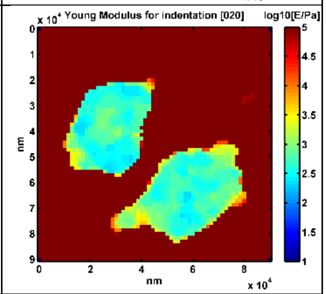  |

| | | |
|---|---|---|
| 10 μM | 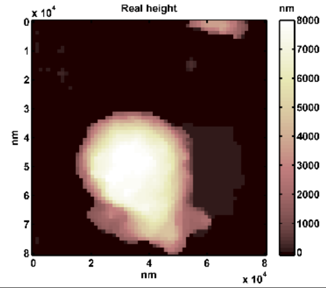 | 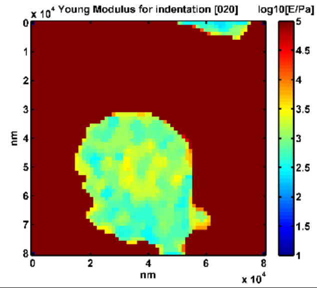 |
| 10 μM | 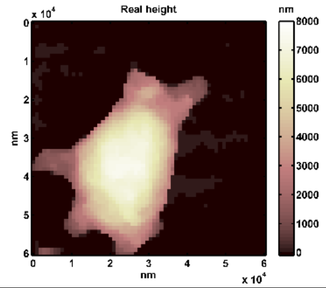 | 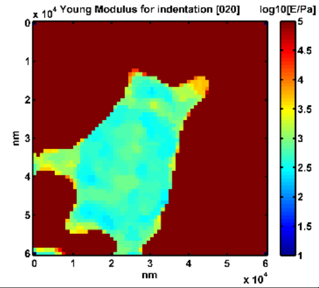 |
| 10 μM | 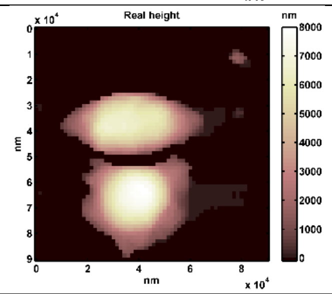 | 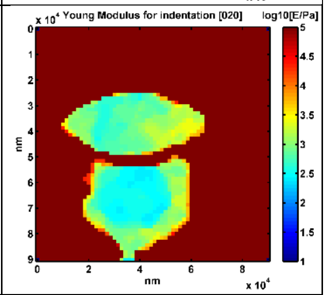 |
| 10 μM | 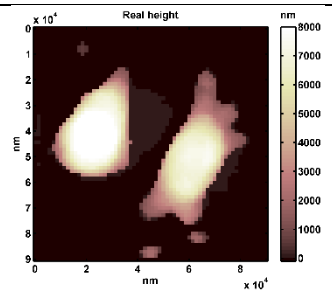 | 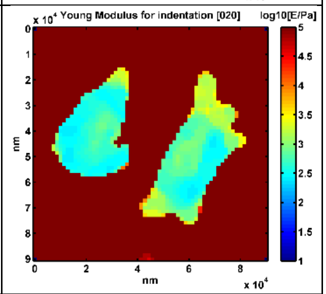 |
| 100 μM | 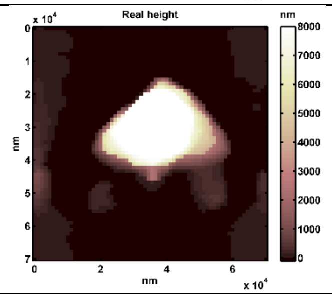 | 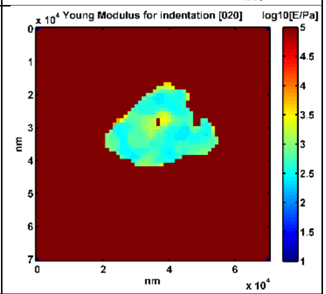 |
| 100 μM | 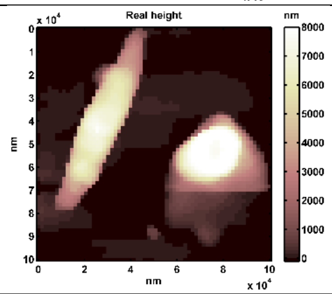 | 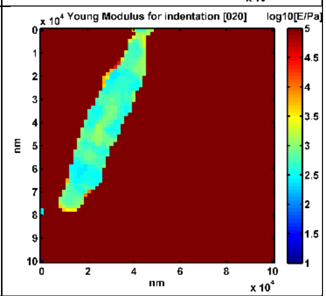 |

100 μM

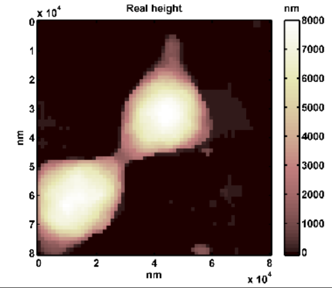


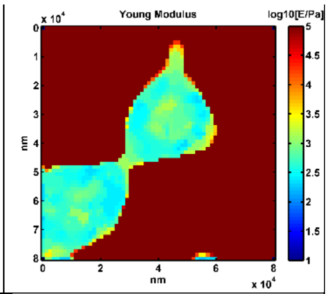


100 μM

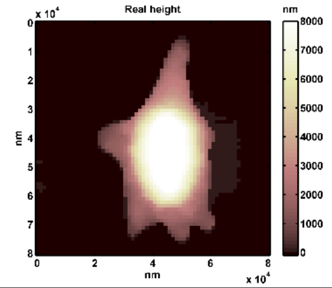


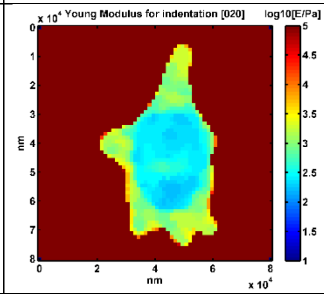


100 μM

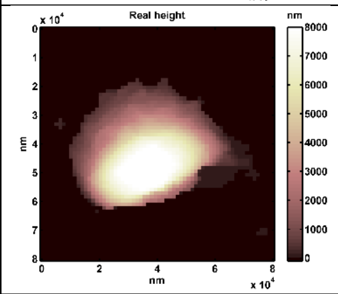


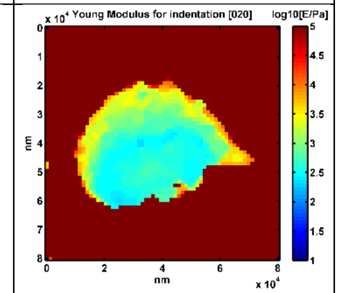


100 μM

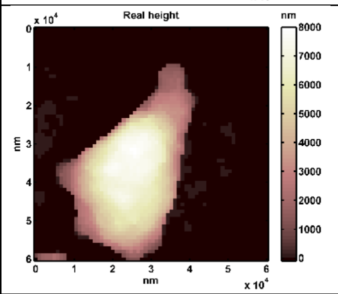


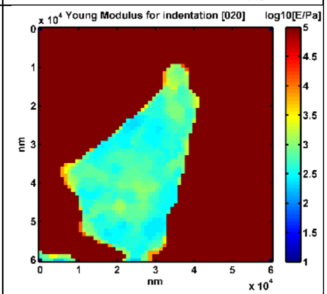


100 μM

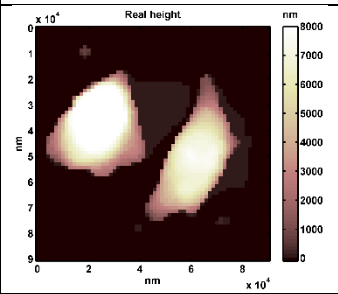


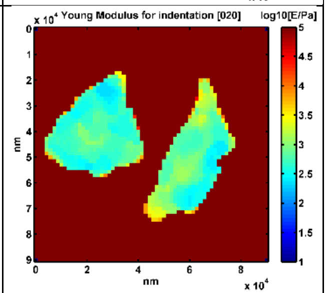


100 μM

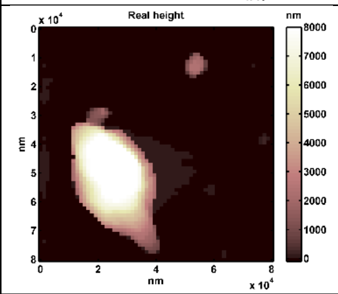


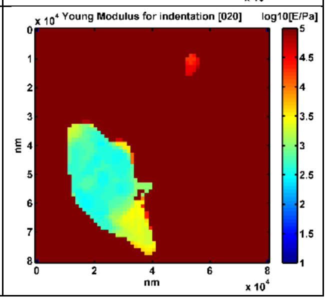

# Bibliography


1. Dimitriadis, E. K.; Horkay, F.; Maresca, J.; Kachar, B.; Chadwick, R. S. Determination of Elastic Moduli of Thin Layers of Soft Material Using the Atomic Force Microscope. *Biophys. J.* **2002,** *82* (5), 2798-2810.
2. Puricelli, L.; Galluzzi, M.; Schulte, C.; Podesta, A.; Milani, P. Nanomechanical and topographical imaging of living cells by atomic force microscopy with colloidal probes. *Rev. Sci. Instrum.* **2015,** *86* (3), 033705.
3. Garcia, M. T.; Gathergood, N.; Scammells, P. J. Biodegradable ionic liquids Part II. Effect of the anion and toxicology. *Green Chem.* **2005,** *7* (1), 9-14.
4. Ranke, J.; Müller, A.; Bottin-Weber, U.; Stock, F.; Stolte, S.; Arning, J.; Störmann, R.; Jastorff, B. Lipophilicity parameters for ionic liquid cations and their correlation to in vitro cytotoxicity. *Ecotoxicol. Environ. Saf.* **2007,** *67* (3), 430-438.
5. Chen, H.-L.; Kao, H.-F.; Wang, J.-Y.; Wei, G.-T. Cytotoxicity of Imidazole Ionic Liquids in Human Lung Carcinoma A549 Cell Line. *J. Chin. Chem. Soc.* **2014,** *61* (7), 763-769.
6. Wang, X.; Ohlin, C. A.; Lu, Q.; Fei, Z.; Hu, J.; Dyson, P. J. Cytotoxicity of ionic liquids and precursor compounds towards human cell line HeLa. *Green Chem.* **2007,** *9* (11), 1191-1197.